



HAL
open science

Oceanic loading monitored by ground-based tiltmeters at Cherbourg (France)

Nicolas Florsch, Muriel Llubes, Guy Wöppelmann, Laurent Longuevergne,
Jean-Paul Boy

► **To cite this version:**

Nicolas Florsch, Muriel Llubes, Guy Wöppelmann, Laurent Longuevergne, Jean-Paul Boy. Oceanic loading monitored by ground-based tiltmeters at Cherbourg (France). *Journal of Geodynamics*, 2009, 48, pp.211-218. 10.1016/J.JOG.2009.09.017. hal-00708017

HAL Id: hal-00708017

<https://hal.science/hal-00708017v1>

Submitted on 14 Jun 2012

HAL is a multi-disciplinary open access archive for the deposit and dissemination of scientific research documents, whether they are published or not. The documents may come from teaching and research institutions in France or abroad, or from public or private research centers.

L'archive ouverte pluridisciplinaire **HAL**, est destinée au dépôt et à la diffusion de documents scientifiques de niveau recherche, publiés ou non, émanant des établissements d'enseignement et de recherche français ou étrangers, des laboratoires publics ou privés.

1 **Oceanic loading monitored by ground-based tilt-meters**

2 **at Cherbourg (France)**

3

4 Nicolas Florsch^(*)⁽¹⁾, Muriel Llubes⁽²⁾, Guy Wöppelmann⁽³⁾, Laurent Longuevergne⁽⁴⁾, Jean-
5 Paul Boy⁽⁵⁾

6

7 (1) UMMISCO/IRD 32, avenue Henri Varagnat 93143 Bondy Cedex, France; UPMC,
8 Paris, France; Dept of Mathematics and Applied Mathematics, UCT, South Africa.

9 (2) Université de Toulouse, OMP 14 av. Edouard Belin, 31400 Toulouse, France

10 (3) LIENSs/ULR, 2 rue Olympe de Gouges, 17000 La Rochelle , France

11 (4) Bureau of Economic Geology, Jackson School of Geosciences, The University of
12 Texas at Austin, PO Box X, Austin, TX 78713, USA

13

14 (5) EOST/IPGS (UMR 7516 CNRS-ULP), 5 rue René Descartes, 67084 Strasbourg,
15 France, and NASA GSFC, Planetary Geodynamics Laboratory, Code 698,
16 Greenbelt, MD 20771, USA.

17

18

19 **Abstract**

20 We installed two orthogonal Blum-Esnoult silica tiltmeters in an underground military facility
21 close to the shore in Cherbourg (France). They have recorded the ocean tide and the
22 associated oceanic loading effects from March 2004 to July 2005. The signal to noise ratio is
23 such that, within a period range from a few minutes to a few days, the main nonlinear oceanic
24 tides up to the M10 group could be observed. The modelling of the tidal tilt deformation has
25 been carried out using oceanic models of the FES2004 family, with a stepwise refinement of
26 the grid size. The comparison with recorded tilt time series shows spectacular improvement
27 when refining the grid and also provides an independent mean to validate the oceanic models
28 and the modelling process. We show that tiltmeters open new opportunities to explore loading
29 of non linear tides on a larger spectrum than gravimeters and GPS do.

30 **Keywords**

31 Inclinerometry, tilt, oceanic loading, FES2004, nonlinear tides

32 **1. Introduction**

33 The oceanic loading phenomenon involves the attraction and deformation of the Earth that are
34 due to the varying weight of moving water masses in the oceans and seas, mainly the oceanic
35 tides. These effects may be measured on the ground by several geodetic observables:
36 classically gravity, land level displacement, (Llubes, 2001, Vey, 2002, Llubes, 2008), but also
37 strain and stress can be used.

38 This paper is focused on to the tilt effects generated by tidal oceanic loading on the French
39 coast (Cherbourg, Cotentin region). The tidal amplitude may reach there up to several meters.

40 While considering gravity variations in the vicinity of a sea with large tides, the proper
41 loading contribution can reach about the third of the elastic earth tide variation (Llubes et al.,
42 2004). Tilts are much more sensitive to the coastal loading because they result mainly from
43 the flexure of the crust, which involves a sensitivity to shorter spatial scales than gravimetry
44 does. Actually the tilt loading itself reaches at Cherbourg about three times the solid tide tilt
45 effect. Precisely, two factors converge to generate a large amplitude to the loading tilt *locally*:
46 1) The decreasing rate of the tilt Green function as a function of the load distance is more
47 rapid with respect to gravity: it behaves as $1/r^2$ instead of $1/r$. This feature leads to a sort of
48 homothetic invariance scale (Rerolle et al., 2006) when integrating over an area which also
49 depends on r^2 ; 2) Coastal areas are zones where the tidal amplitude is much greater than in the
50 open ocean. Finally, these properties make the tiltmeters highly sensitive and suitable to
51 study local loading phenomena.

52 Strictly speaking, tiltmeters record the variations of the gravity direction, more precisely the
53 variations between the instantaneous geoid and the crust on which these instruments are
54 settled. Both are affected by water loads. In practical terms, the only signal that can be
55 reached is the difference between the geoid and the crust. It is not possible to refer tilts to a
56 space or terrestrial reference frame because the accuracy that would be required to refer tilt
57 data to this frame should be of the same order of magnitude than a tiltmeter resolution (at
58 least), that is better than 10^{-9} at short time scale (a few seconds). Of course, it is only a
59 practical limitation. Actually, the zero instrumental reference is just its initial state when
60 beginning the record.

61 The geometrical and dynamical effects induced by the oceanic loads can be easily computed
62 using the Green formalism, which degenerates in a simple convolutive formalism as long as
63 the Earth is considered as spherically symmetric. Green functions describe the linear elastic
64 Earth response to a local load in terms of vertical and horizontal displacements, stress, strain,

65 gravity... Tilt Green functions can be found in Pagiatakis (1990). See also Boy et al. in this
66 issue.

67 **2. Experiment description and site corrections**

68 **2.1. Tiltmeters records**

69 The tiltmeters used in this experiment are very compact instruments historically designed by
70 Blum (1962) (see also Saleh, 1991) and nowadays built by Marie-France Esnault at IPGP.
71 These instruments are made with silica glass and is built according to Zöllner's pendulum
72 concept. Tiltmeters require a two-step calibration: the first one is electronic (the sensitivity of
73 the displacement probe) and the second one is purely mechanistic (the amplification of a
74 pendulum is $1/\sin(\alpha)$, α being the angle between the rotation axe and the vertical line).
75 Scientific and historical background of this kind of probes may be found in Melchior (1983).
76 Braitenberg et al. (1999) also provide a suitable summary of their functioning.

77

78 The tiltmeters used in this experiment can reach a resolution of about 10^{-9} rad. Actually the
79 gain accuracy (calibration constant) is expected to be better than 4 % (at 1σ). However,
80 pendulums are affected by some "external" limitations. They are highly sensitive to very local
81 environmental background variations: temperature, humidity of the supporting materials, and
82 any kind of natural or induced deformation of the stand. For instance, assuming a 30 cm
83 baseline tripod, a 1 micrometer stem vertical displacement would lead to a $3 \cdot 10^{-6}$ rad tilt
84 effect. Generally speaking, a noticeable drift is observed on that kind of instruments, which is
85 rarely understood in details. This drift could also involve the creeping of the tiltmeter
86 components themselves: it is worth mentioning that 10^{-9} rad variation over a 30 cm baseline is
87 less than the elementary quartz crystal size. Hence, a suitable efficiency can only be reached

88 thanks to exceptional settling conditions. In our experiment, two orthogonal pendulums have
89 been installed in an unused part of a military underground installation owned by the French
90 Marine, the “Souterrain du Roule”, at Cherbourg (Figure 1). A drift does actually exist on
91 both tiltmeters directions (EW and NS). However, it only causes interferences within the long
92 period variations (saying, more than a week), which can be eliminated by standard filtering
93 methods to focus on the diurnal tidal band and its harmonics without spectral windowing
94 artefacts.

95 **2.2. Site effects**

96 Site effects include both topographic and cavity effects. Both deform the local stress field and
97 so they modify (magnify or reduce) the targeted tilt signal. Harrison (1976) was the first to
98 provide a useful approach to deal with such undesirable effects. He clearly showed the major
99 influence of the topography: in the core of a hill, the tilt could be changed by a large factor
100 (from 0.25 to 10 outdoor in a talweg). An essential characteristic of site effects is the relative
101 phase shift with respect to its theoretical value, which can reach as much as 40° (Lecolazet
102 and Wittlinger, 1974).

103 The paper by King *et al.* mentions two issues to correct the site effects: first the practical
104 problem of constructing and checking large three-dimensional models, and second the
105 difficulties of obtaining the correct input data for the models. Nowadays, Finite Element
106 Method (FEM) could be applied (see for instance Kroner *et al.* 2005). However, in our case it
107 will not be very useful. These authors also remind us Itsueli *et al.* work (1975) in which the
108 problem of the existence of surrounding fracture - that are not well mapped introduces
109 additional difficulties. They proposed a method for removing the site effects without recourse
110 to modelling by using a response method actually based on the seismic response or Raleigh
111 waves. Neither of these methods can be used here. As stated by King *et al.* (1976) the first

112 method is valid only for sites distant from ocean loading and the second requires at least the
113 vertical component which is not available in our case.

114 However two points must be emphasised to lower the site effects. Firstly, body forces are
115 generally considered to study cavity effects, whereas the study of the crust flexure results
116 from remote surface loads. Potential site effects are reduced to a shear effect alone. Here, the
117 direct Newtonian attraction is lowered (water masses are more or less at the same altitude than
118 the instrument) –however, the mass redistribution potential (and forces) cannot be neglected.
119 Secondly, tiltmeters have been installed more or less in the middle of the tunnel (a symmetry
120 axis), where the disturbing effect is supposed to vanish.

121 The solution we finally adopted consists in dropping potential site effect corrections,
122 assuming it is less critical than in the frame of a body Earth Tide study. Finally, remembering
123 that Lecolazet and Wittlinger (1974) associated a significant phase to cavity effect, we state
124 that the undetectable phase difference between the observed and the modeled tidal tilt
125 variations will be an a-posteriori justification of the reduced rule of site effect.

126 **2.3. Atmospheric contribution on tilt.**

127 The atmosphere contributes to the tilt as any other moving mass (Boy *et al*, this issue). Two
128 deformation processes have to be modeled: direct attraction (modifying the equipotential),
129 and the elastic deformation due to the additional pressure on the crust, which also implies
130 mass redistribution and thus an effect on the geoid (Farrell, 1972). The formalism to compute
131 the atmospheric contribution is similar to those used in the oceanic or continental
132 (hydrological) loading problems, except that one should consider here that the station is inside
133 the atmosphere shell. As in the hydrological case, tilts are only influenced by the spatial
134 pressure gradient (Rerolle *et al.*, 2006). It implies that the classical admittance method cannot
135 be used in our case. Two methods can be used to correct the atmospheric pressure

136 contribution. One would use a local barometer network, which would require a heavy
137 installation structure because of the different spatial scales involved in the deformation. A test
138 was carried out, but did not provide good results. Moreover, the pressure effect on that coastal
139 border is complicated by the dynamic response of the ocean. The second method consists in
140 using the atmospheric data as provided by meteorological models. Unfortunately, the
141 sampling rate of these is too coarse, and does not allow to study phenomena below 12 hours.
142 On a spectral point of view, pressure effects induce a rosy noise superimposed with periodic
143 signals. If a good atmospheric pressure correction is expected to improve the S/N ratio, we
144 suspect that it would be a real but light improvement in our spectral analysis. Finally, we
145 dropped this correction since no data is available within the given frequency range.

146 Traditional Earth Tide (ET) studies have benefited from gravity observations, such as the
147 GGP experiment (<http://www.eas.slu.edu/GGP/ggphome.html>). Most of the geodesists
148 consider that the discrepancies between the observations and the models are very tiny.
149 Actually, they are much smaller toward the inner continental stations where the influence of
150 oceanic loadings is reduced. The agreement between the Love numbers used to compute Earth
151 elastic tides and the GGP cryogenic gravimeter data is better than 1/100. This is indeed
152 negligible when considering the factor calibration accuracy and one can assume that the
153 modelled Earth tide elastic contribution is very accurate and can be subtracted from the raw
154 data to leave only oceanic loading effects. However, the situation is not so simple if we
155 remind the nature of the site effect. Here, an “exact tide” is subtracted from a signal where the
156 tides could have been multiplicatively changed by the site magnification. Hence, the
157 legitimacy to remove the elastic tide lies on the fact that i) it is smaller than the loading, ii)
158 the site effect factor is not too far from 1 (due to the location of the probes near the center of
159 the tunnels). The combination of these two “small” hypothesis let us hope that these
160 approximations are not too dramatic, although it is not possible to estimate them with

161 accuracy. Finally, we consider that the error associated with site effects is reduced due to (1)
162 the position of the tiltmeters in the center of the tunnel and (2) the reduced amplitude of the
163 Earth Tide by a factor 5 with respect to loading.

164 **3. Signal processing and spectral analysis.**

165 **3.1 Basic spectral analysis**

166 Tilts were initially sampled at 30 sec intervals. We applied high-pass filtering (to remove the
167 drift) and resampling (with low-pass filtering to avoid aliasing). This finally restricts the
168 bandwidth to the useful periods between 10minutes and 72 hours. Raw and filtered signals are
169 plotted on Figure 2. The amplitude spectra of the filtered signals are plotted on Figure 3. We
170 chose a spectral normalization which preserves the amplitude of the periodic signal rather
171 than the density power spectrum. Hence, the tidal wave amplitudes can be directly read in
172 microradians.

173 The spectra show several harmonics of the diurnal tidal waves. They are directly linked to the
174 non-linear hydrodynamical waves in the English Channel (and do not result from any kind of
175 non-linearity of the Earth elastic response). The most further way to model the observed
176 amplitude requires to compute these non linear waves by using the most complete oceanic
177 charts (involving hydrodynamic modelling plus data assimilation) and to combine them with
178 the rheological response of the Earth (convolutive or more sophisticated). However, the
179 difficulties of getting upper order waves lies in the mesh definition and restitution as seen by
180 altimetric satellites, more exactly it depends on the trade-off between time and space
181 sampling, both limited in practice (Cartwright and Ray, 1990). This becomes more and fussier
182 as the order increases, since the higher the order, the smaller the typical wavelength to be
183 taken into account.

184 Several points should be highlighted here:

- 185 - the amplitude of even orders is greater than for other harmonics. This is expected
186 since they are successive harmonics of the M2 dominant group.
- 187 - Tiltmeters are able to record nonlinear waves up to 8 cycle/day. Note that neither
188 loading gravity studies (Boy *et al.*, 2004) nor any other integrative geodetic method
189 have been able to “see” these higher harmonic signals (although they are clearly seen
190 in tide gauge records, of course). Hence tiltmeters turns out to be very sensitive tools
191 to observe the deformation induced by the oceanic tides at the regional scale.

192

193 **3.2. Tidal analysis**

194 Earth tide analysis softwares are designed to estimate the transfer response of the Earth with
195 respect to the astronomical gravity potential, usually providing the delta and gamma factors
196 (Melchior, 1983). To search for higher tidal harmonics in the tiltmeter records, we therefore
197 looked for tidal analysis tools which actually are standard within the sea-level community.
198 We used the MAS software developed by Simon (2007) which implements a general method
199 for analysing sea level heights. Pouvreau *et al.* (2006) compared MAS to the well-known and
200 widely distributed T_TIDE software (Pawlowicz *et al.* 2002), and could not notice any
201 significant difference from both sets of estimated tidal amplitudes at Brest. A drawback of the
202 current T_TIDE release is, however, that it cannot analyse datasets longer than one-year,
203 whereas MAS is successfully applied over periods even longer than a century.

204 Table 1 shows the main tidal constituents that we obtained from the ocean-like tidal harmonic
205 analysis performed on the tiltmeter observations that were previously corrected from the Earth
206 tides over the period 2004/03/09 to 2005/07/18. The units are expressed in nano-radians.

207

208 **3.3 FES2004/NEA time modelling and sensitivity test distance**

209 The modelling is performed by combining FES2004 global oceanic model (Lyard *et al.*
210 2004), and the refined NEA (North East Atlantic tidal solution) model in the close Atlantic
211 and English Channel (Pairaud *et al.*, 2008).

212 We have plotted on figure 4 the modelled oceanic loading and the Earth Tide contribution, as
213 well as the sum of these two signals and compared them with the observation. The chosen
214 window permits to illustrate the best and the worst agreement. The largest discrepancies
215 between modelled and observed oceanic loading occur for large tidal ranges. At the end of the
216 window, during during small tidal ranges, the agreement is far better (the whole time-series is
217 available on request). In general, the EW component is better modelled than the NS
218 component. This may be linked to the coast orientation (EW) which is located 2km
219 northwards of the observing site.

220 We do not know the origin of these discrepancies and their variations in time. However, we
221 form the hypothesis that it could come from the interference arrangement between the main
222 tidal M2 group and the overtones (nonlinear harmonics). We only took into account 8 waves
223 in the diurnal and semi-diurnal bands here and none of the non-linear tides. A further check
224 will require to model the whole M4 group and even upper modes.

225 **Test distance**

226 We tested the spatial sensitivity of the tiltmeters. We have chosen an adapted geographical
227 windowing, as in Boy *et al.* (2003) to represent the different contribution of several areas.
228 This method splits the oceanic contribution into parts according to an adequate division of the
229 geographical areas. The relevance of these areas is linked to the specificity of the local and
230 regional coast contouring. The choice of the zones is partially arbitrary and is only for

231 discussion, but fundamentally also depends on the sensitivity of the method with respect to
232 the distance, and hence on the power behaviour of the Green function: $1/r$ for gravity and $1/r^2$
233 for tilts.

234 Three zones were considered (see Figure 5):

- 235 - Z1 corresponds to the English Channel (based on NEA model)
- 236 - Z2 delimitate an intermediate zone (also based on NEA model)
- 237 - Z3 is for the other parts of the world (using FES2004)

238 Figure 5 also shows M2 wave amplitude. Figure 6 shows the cumulative contributions of each
239 of these 3 zones for all the diurnal and semi-diurnal waves.

240 In the semi-diurnal band (N2, M2, S2 and K2), we observe the effect of the local
241 magnification of the corresponding group periods. Large zooms are required to see the further
242 contribution; the local signal is definitely dominant.

243 The diurnal waves (O1, P1, K1, Q1) form a second class of patterns. Though the local zone
244 (English Channel) dominates the signals, the Atlantic and remote zones are almost of the
245 same order of magnitude and none of the contribution could be neglected. This is due to the
246 fact that the diurnal waves are not amplified by the Channel

247 **Discussion and Conclusions**

248 The sensitivity of the tilt method allows to observe the loading effect with a high signal/noise
249 ratio. This implies that assuming a known mechanical response of the Earth, tiltmeters can be
250 used to validate oceanographic models and nonlinear tides. Contrary to tide gauges whose
251 spatial sensitivity is strictly local (and can be affected by the port configuration), the tilt offers
252 an integrative measurement of the behaviour of the ocean with a regional spatial sensitivity.

253 They even could be more sensitive to coastal zones when tidal waves are magnified. This is
254 the case for the M2 group; the wave amplitude is quickly decreasing when the distance to the
255 coast increases, making the remote contribution really negligible.

256 The four main remaining issues are: 1) the difficulty to achieve a good accuracy in the
257 calibration factor for this kind of tiltmeters, 2) the site effect, which is difficult to estimate in
258 most cases, 3) the lack of atmospheric detailed data to correct from pressure within this short
259 period band, and 4) the necessity to take into account a dynamical and coupled atmosphere-
260 ocean modelling (see Boy *et al.*, this issue). However, these issues can be tackled in a near
261 future. New experiments are carried on in Brittany near Ploemeur in France (Bour *et al.*,
262 2008) which could serve to improve our knowledge. Indeed, long-base hydrostatic tiltmeters
263 have been set up in shallow galleries. They have been recording for a few months. Both
264 calibration uncertainties and site effects will be easier to solve there for that kind of
265 instruments. In parallel, atmospheric sampling rates and coupled modelling with the oceans
266 are continuously improving.

267 Due to its features and assuming further improvements, tilt could become a systematic tool to
268 test oceanic models as far as non linear high harmonics are concerned. Neither gravity nor
269 GPS techniques are able to see M4, M6, M8 and M10 waves with such a signal/noise ratio as
270 the one reached by tiltmeters today.

271 **Acknowledgement**

272

273 We thank Marie-France Esnault and Karim Mahiouz for installing the tilt-meters, Jacques
274 Delorme and the French Marine for providing the Roule gallery to install the tilt-meters. We
275 would also like to thank Bernard Simon (SHOM) for kindly providing us his tools (MAS) in
276 order to apply the ocean tidal-like analyses to the tiltmeter records. This study has been

277 supported by the program CNRS-DBT and the grant in the frame of the multi-organisation
278 GDR-G2. Nicolas Florsch is currently welcomed at the Department of Mathematics and
279 Applied Mathematics at Cape Town University, South Africa, and is granted by the French
280 Organization “Institut de Recherche pour le Développement”. Jean-Paul Boy is currently
281 visiting NASA Goddard Space Flight Center, with a Marie Curie International Outgoing
282 Fellowship (N° PIOF-GA-2008-221753).

283 **References**

284 Blum, P., 1962. Contribution à l'étude des variations de la verticale en un lieu, *Ann.*
285 *Geophys.*, 19, 215–243.

286 Boy, J.P., Llubes, M., Hinderer, J., and Florsch, N., 2003. A comparison of tidal ocean
287 loading models using superconducting gravimeter data. *JGR*, vol. 108, n°B4.

288

289 Boy, J.-P., M. Llubes, R. Ray, J. Hinderer, N. Florsch, S. Rosat, F. Lyard and T. Letellier,
290 2004, Non-linear oceanic tides observed by superconducting gravimeters in Europe, *J.*
291 *Geodyn.*, 38, 391-405.

292

293 Braitenberg.C., and Zadro, M., 1999. The Grotta Gigante horizontal pendulums -
294 instrumentation and observations. *Bollettino di Geofisica Teorica ed Applicata*, 40 , no 3-4,
295 pp. 577-582.

296

297 Cartwright, D.E., and Ray, R.D., 1990. Oceanic tides from Geosat altimetry. *J. Geophys.*
298 *Res.*, 95 (C3), pp. 3069–3090.

299

300 Farrell, W., 1977. Deformation of the Earth by surface load, *Review of Geophysics Space*
301 *Physics*, 10(3), 761–797.

302 Harrison, J. C., 1976. Cavity and topographic effects in tilt and strain measurements. *J.*
303 *Geophys. Res.*, 81, 319 – 328

304

305 Itsueli, U.J., Bilham, R.G., Goult, N.R., and King, G.C.P., 1975. Tidal strain enhancement
306 observed across a tunnel, *Geophys. J. R. astr.Soc.*, **42**, 555

307

308 King, G., Zürn, W., Evans, R., Emeter, D., 1976. Site Correction for Long Period
309 Seismometers, Tiltmeters and Strainmeters. *Geophysical Journal International*, vol. 44, issue
310 2, pp. 405-411.

311 Kroner, C., Jahr, T., Kuhlmann, S., & Fisher, K., 2005. Pressure-induced noise on horizontal
312 seismometer strainmeter records evaluated by finite element modelling, *Geophys. J. Int.*, 161,
313 167–178.

314 Lecolazet, R. & Wittlinger, G., 1974. Sur l'influence perturbatrice de la deformation des
315 cavités d'observation sur les marées clinométriques, *C. R. Acad. Sc. Paris*, 278, 663–666.

316 M. Llubes, N. Florsch, J.P. Boy, M. Amalvict, P. Bonnefond, M.N. Bouin, S. Durand, M.F.
317 Esnault, P. Exertier, J. Hinderer, M.F. Lalancette, F. Masson, L. Morel, J. Nicolas, M.
318 Vergnolles, G. Wöppelmann, 2008. Multi-technique monitoring of ocean tide loading in
319 Northern France. *Compte-rendus Géosciences*, C. R. Geoscience 340, 379–389

320

321 Llubes, M., Florsch, N., , Amalvict, , M., Hinderer, J., Lalancette, M.F., Orseau, D., et Simon,
322 B., 2001. Observation gravimétrique des surcharges océaniques : premières expériences en
323 Bretagne. *C.R. Acad. Sci, Earth and Planetary Sciences* 332, 77-82.

324 Melchior, P., 1983. The Tides of the Planet Earth, Pergamon Pr.

325 Pagiatakis, S., 1990. The response of a realistic Earth to ocean tide loading, *Geophys. J. Int.*,
326 103, 541–560. DOI: 10.1111/j.1365-246X.1990.tb01790.x

327 Pawlowicz, R., Beardsley, B., and Lentz, S., 2002. Classical tidal harmonic analysis error
328 estimates in MATLAB using T_TIDE. *Comput. Geosci.* 28, 929–937.

329 Pouvreau, N., Martin Miguez, B., Simon, B, and Woppelmann, G., 2006. Evolution of the
330 tidal semi-diurnal constituent M2 at Brest from 1846 to 2005. *C. R. Geoscience*, 338, pp.
331 802–808.

332 Rerolle, T. , Florsch, N., Llubes, M., Boudin, F., and Longuevergue, L., *Inclinometry, a new*
333 *tool for the monitoring of aquifers? C. R. Geoscience* 338 (2006).
334 [doi:10.1016/j.crte.2006.07.004](https://doi.org/10.1016/j.crte.2006.07.004)

335 B. Saleh, P.A. Blum and H. Delorme, New silica compact tiltmeter for deformations
336 measurements, *J. Survey Eng.* 117 (1991), pp. 27–35.

337 Simon, B, 2007. *La marée océanique côtière. Collection “Synthèses”*, Ed. Insitut
338 Océanographique, 433 pp.

339

340 Vey, S. , Calais, E., , Llubes, M., Florsch, N., Woppelmann, G., Hinderer, J., Amalvict, M.,
341 Lalancette, M.F., Simon, B., Duquenn F., Haase, F.S., 2002 GPS measurements of ocean
342 loading and its impact on zenith tropospheric delay estimates: a case study in Brittany,
343 France. *Journal of Geodesy*, vol. 76, 8, pp 419-427.

344

345

346 **Figure captions:**

347

348 Figure1 : Site location and installation of a Blum Pendulum in the “Souterrain du Roule” at

349 Cherbourg

350

351 Figure2 : EW and NS raw and band-pass filtered tilt records at Cherbourg

352

353 Figure 3 : Fourier analysis (periodogramms) of the tilt records reveal a high signal/noise ratio
354 of 100 (40 dB) at 2 cycle/day. It detect peaks till the 1/10 diurnal cycle.

355

356 Figure 4: on the bottom part, Earth tide and loading models are shown separately, while there
357 are summed in the top part of the figure. In both cases, the observation is also plotted and
358 shows a greater amplitude than the model. The misfit could be due to non-linear tides that are
359 not included in this computation.

360

361 Figure5 : The computation is performed by distinguishing three exclusive zones: this enables
362 to study the influence of close, intermediate and distant oceanic loading effects. Zone 1: from
363 -5° to 1.5° in long and 48.5° to 51.25° in lat; Zone 2: from -20° to 14° in long and 30° to
364 61° in lat (excluding Z1); Zone 3: global excluding Z1 and Z2. In Z1 and Z2 the North-East
365 Atlantic (NEA) tidal solution (Pairaud et al., 2008) is used, while Z3 is computed by using
366 FES2004 model (Lyard et.al., 2006).

367

368 Figure 6: Cumulative contribution of the 3 different zones for all diurnal and semi-diurnal
369 waves.

370

371 Table 1 : Results from the ocean-like tidal harmonic analysis applied to the tiltmeter
 372 observations (2004/03/09-2005/07/18) previously corrected for the Earth tides.

Tidal constituent	ALPHABETICAL DOODSON NR.	Amplitude East-West (in nano-radians)	Amplitude North-South (in nano-radians)
M2	<i>BZZZZZZ</i>	435	404
S2	<i>BBXZZZZ</i>	149	141
N2	<i>BYZAZZZ</i>	85	82
K2	<i>BBZZZZZ</i>	41	40
K1	<i>AAZZZZA</i>	34	23
O1	<i>AYZZZZY</i>	19	6
P1	<i>AAXZZZY</i>	11	6
Q1	<i>AXZAZZY</i>	1	10
M4	<i>DZZZZZZ</i>	12	32
MS4	<i>DBXZZZZ</i>	8	20
MN4	<i>DYZAZZZ</i>	4	10
M6	<i>FZZZZZZ</i>	3	7
2MS6	<i>FBXZZZZ</i>	3	8
2MN6	<i>FYZAZZZ</i>	2	5
5MS8	<i>HXBZZZZ</i>	1	6

Figure 1

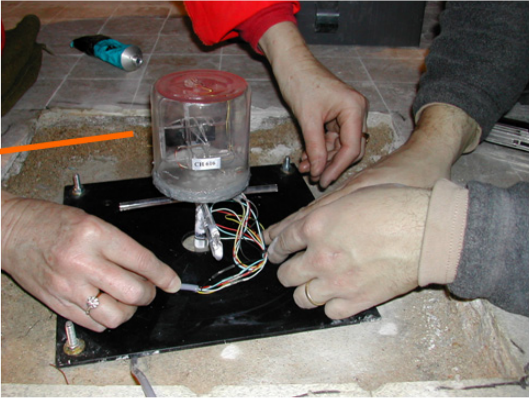


Figure 2 :

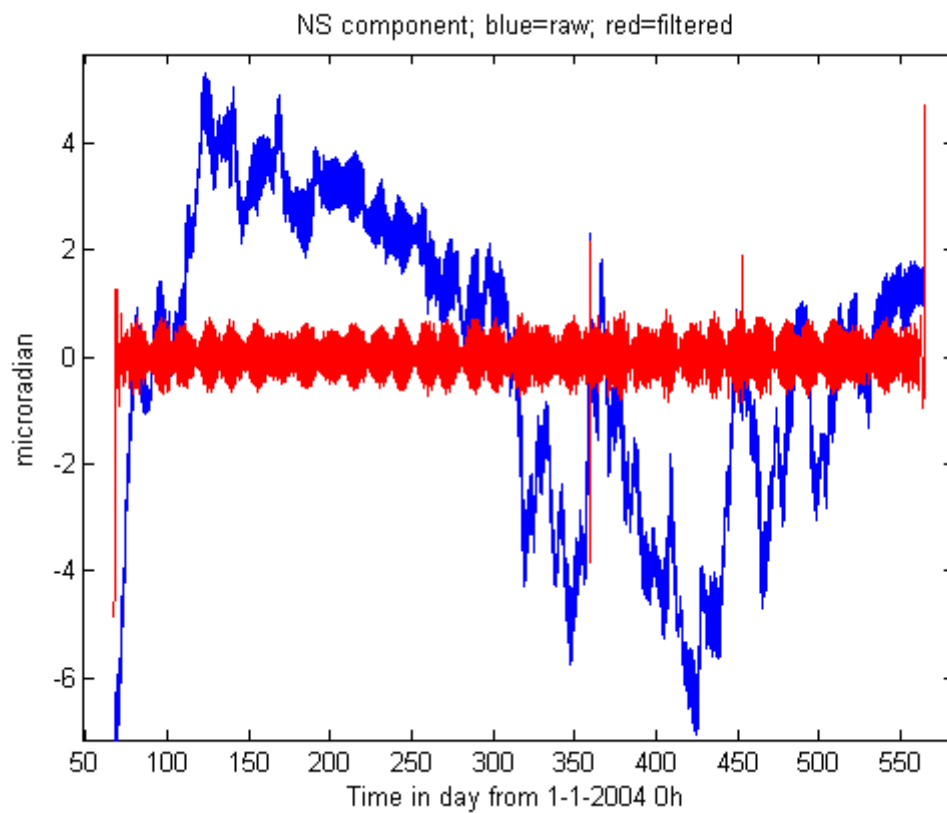
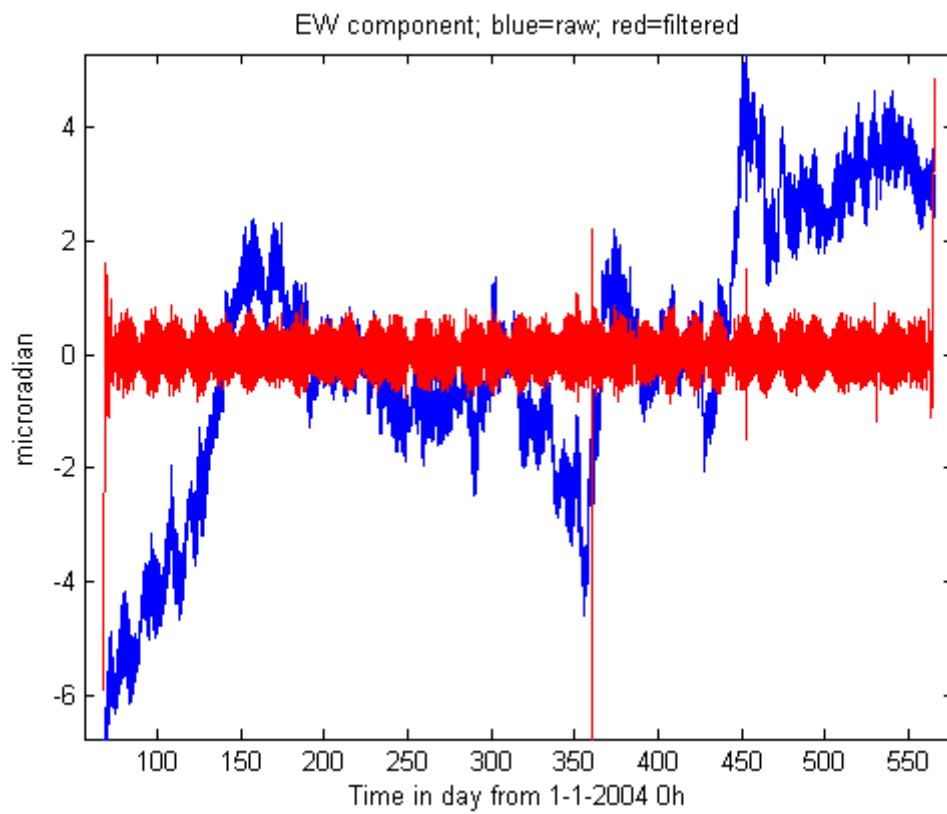


Figure 3

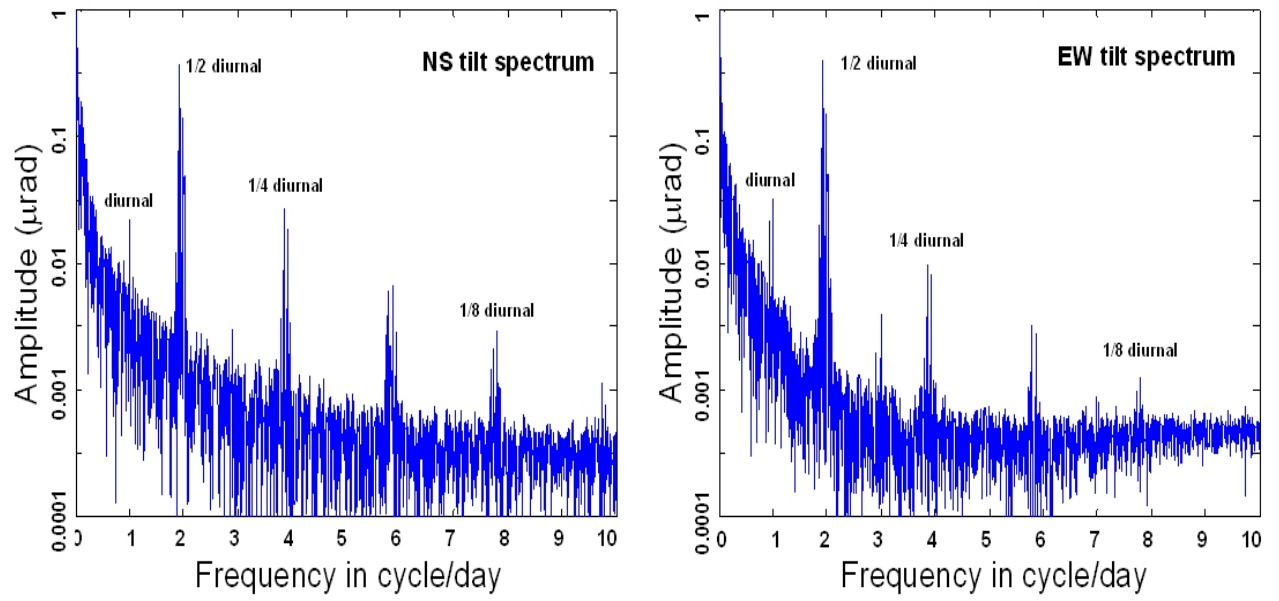


Figure 4

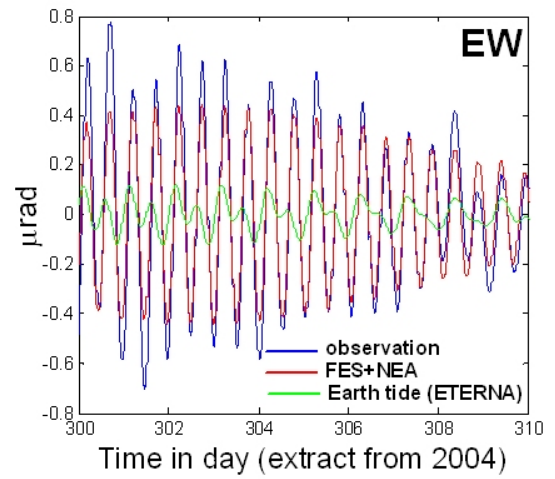
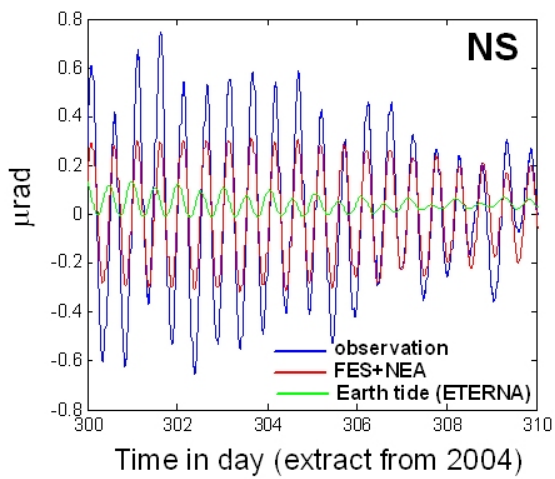
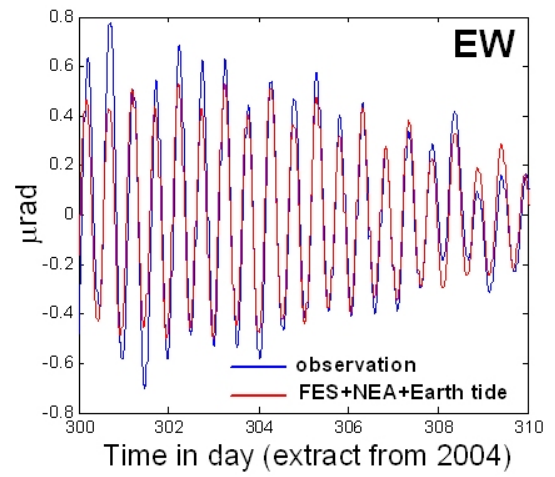
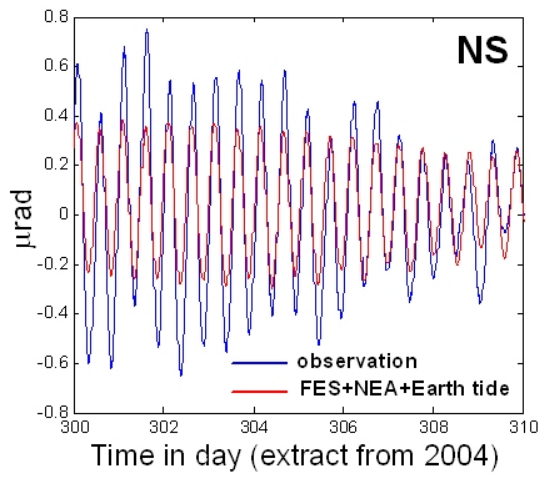


Figure 5

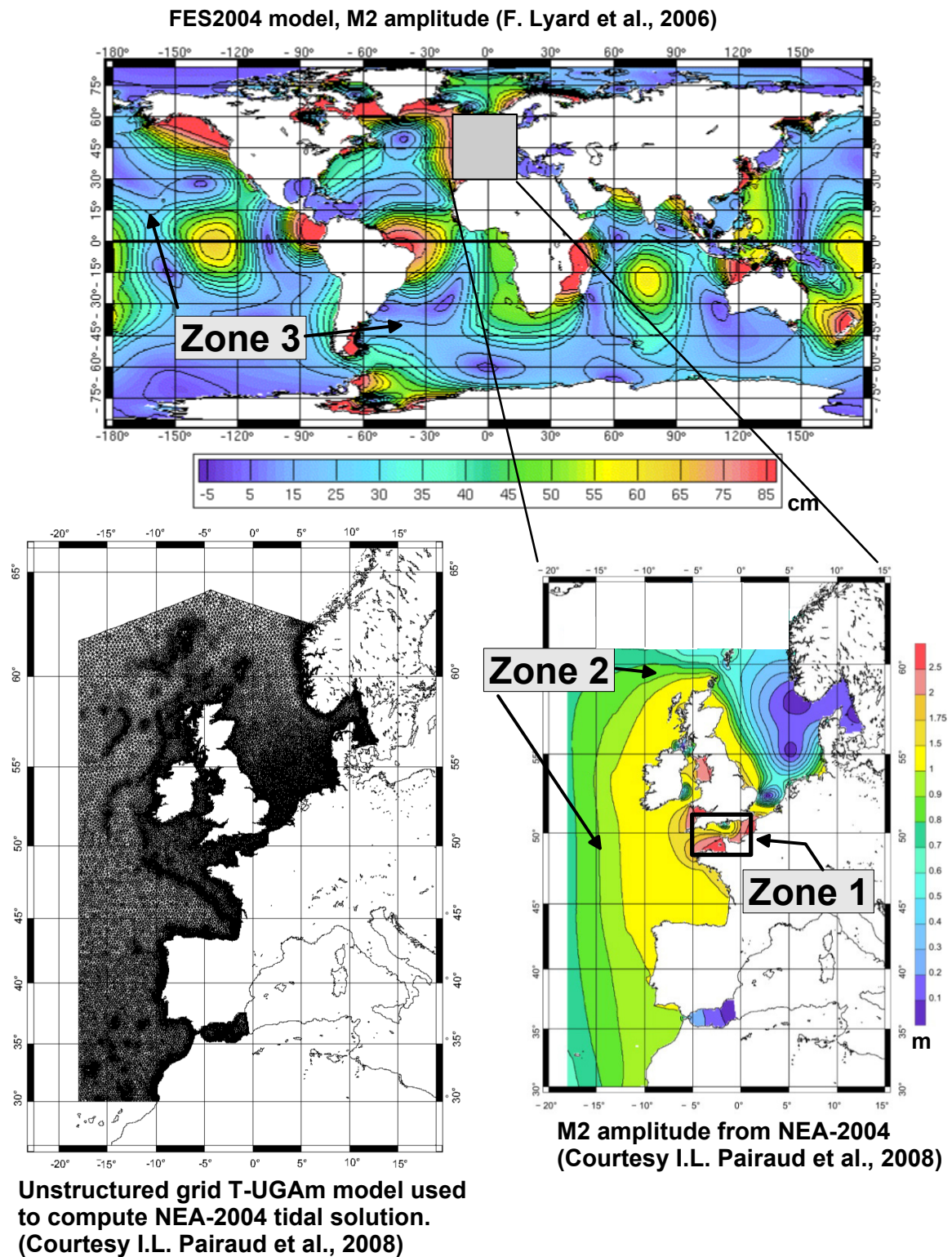


Figure 6

